

Обзор ArXiv:astro-ph, 21-25 марта 2016 года

От Сильченко О.К.

Astro-ph: 1603.05881

**Gas dynamics and outflow in the barred starburst galaxy NGC
1808 revealed with ALMA**

Dragan Salak

*Department of Physics, School of Science and Technology, Kwansei Gakuin University,
Gakuen 2-1 Sanda, Hyogo 669-1337, Japan*

`d.salak@kwansei.ac.jp`

Naomasa Nakai and Takuya Hatakeyama

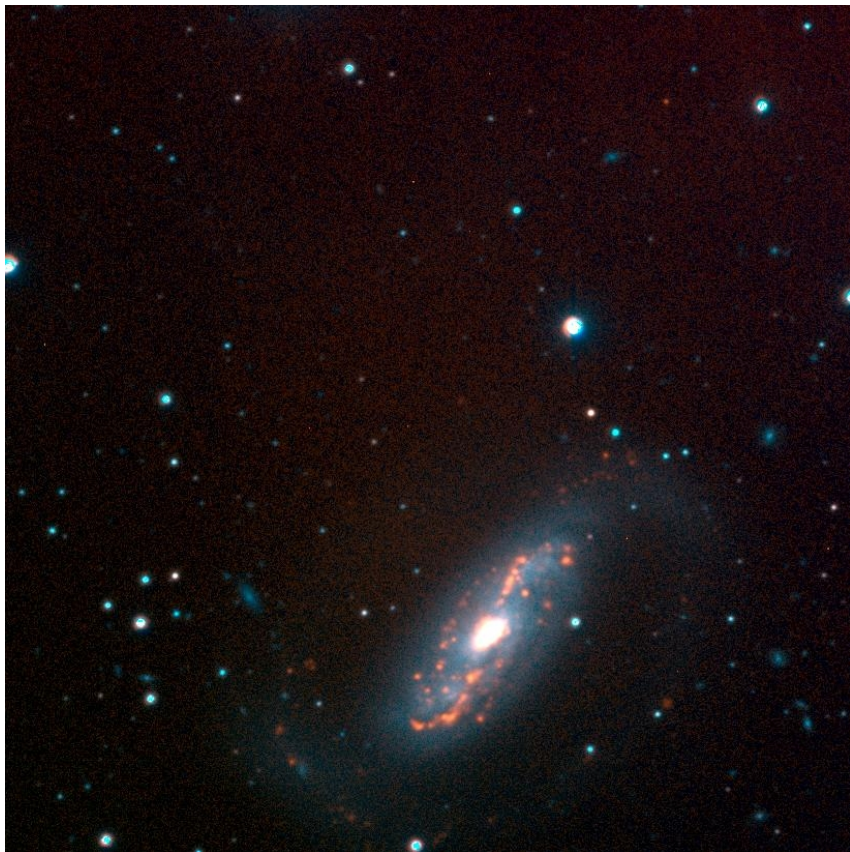
*Division of Physics, Faculty of Pure and Applied Sciences, University of Tsukuba,
Tennodai 1-1-1, Tsukuba, Ibaraki 305-8571, Japan*

and

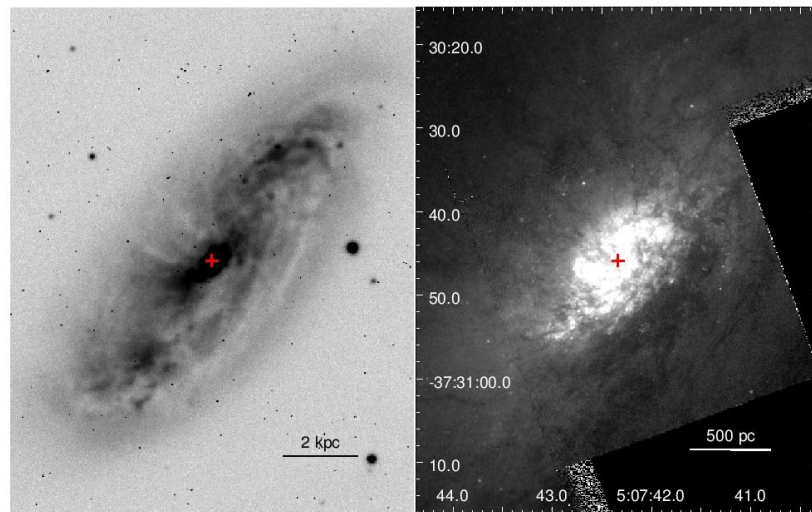
Yusuke Miyamoto

*Nobeyama Radio Observatory, National Astronomical Observatory of Japan, 462-2
Nobeyama, Minamimaki, Minamisaku, Nagano 384-1305, Japan*

(R')SABb NGC 1808



H-alpha



R

HST

ALMA: карты CO и поле скоростей молекулярного газа

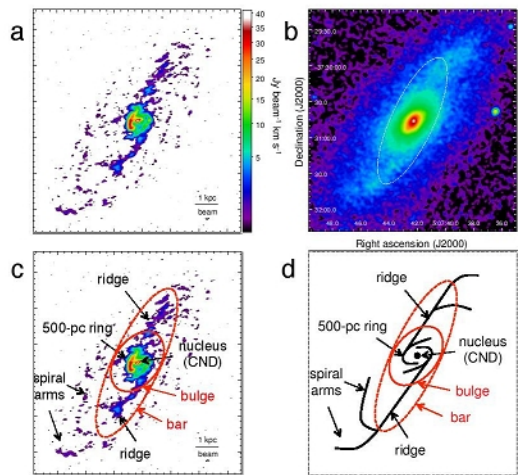
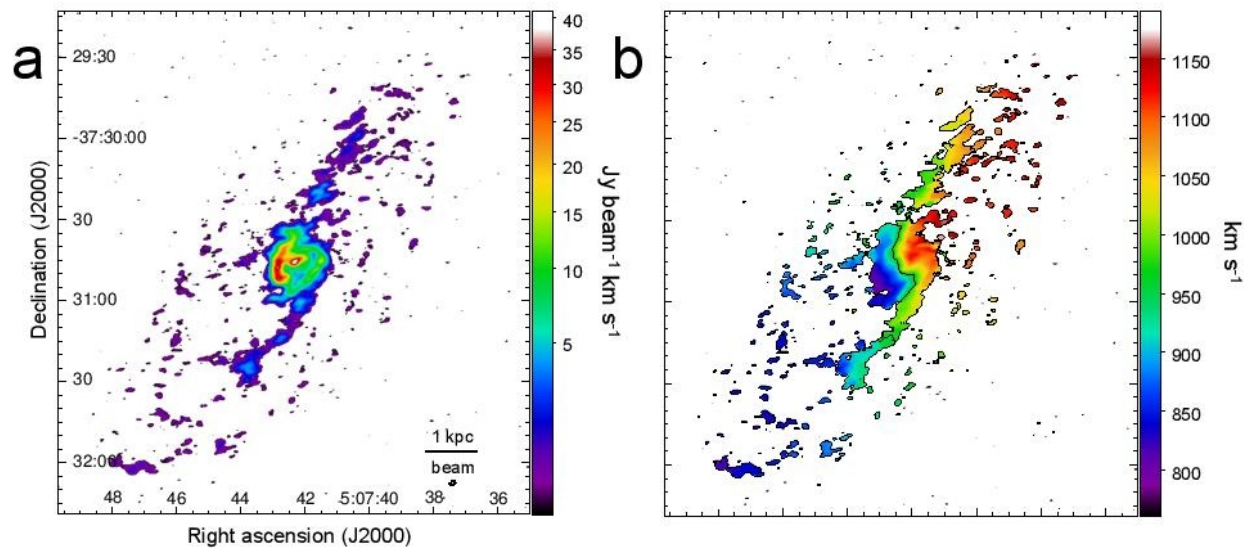


Fig. 7.— (a) High-sensitivity image of CO (1-0) integrated intensity (moment 0) presented on a square root scale from $0.22 \text{ Jy beam}^{-1} \text{ km s}^{-1}$ (pixels below 4σ , where $1\sigma = 5.5 \text{ Jy beam}^{-1}$, were masked) to the peak value of $41 \text{ Jy beam}^{-1} \text{ km s}^{-1}$. The synthesized velocity map ($2''.55 \times 1''.41$ at $PA = -82^\circ$) is shown at the lower right corner. (b) 2MASS image in K_s -band



Радиальное распределение плотности молекулярного газа

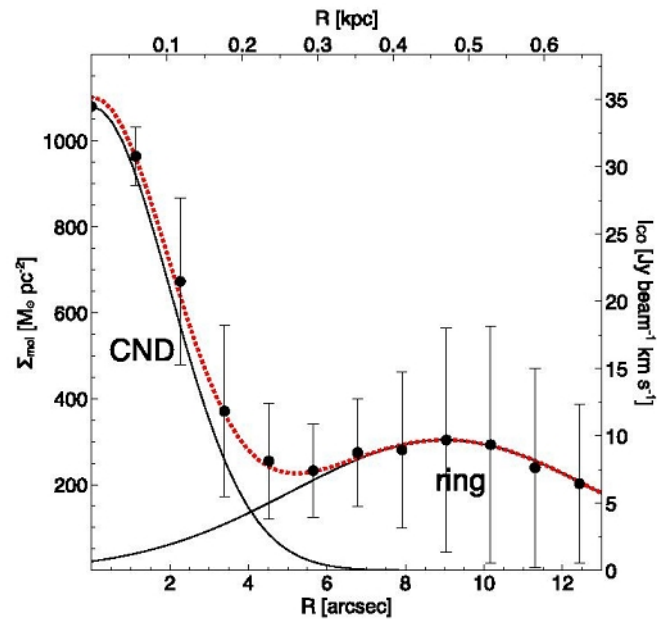


Fig. 11.— Molecular gas surface density (or integrated flux density) averaged over azimuth as a function of radius, $\Sigma_{\text{mol}}(R)$. The data are fit with two Gaussian functions representing the circumnuclear disk (CND) and the 500-pc ring.

Динамическая модель

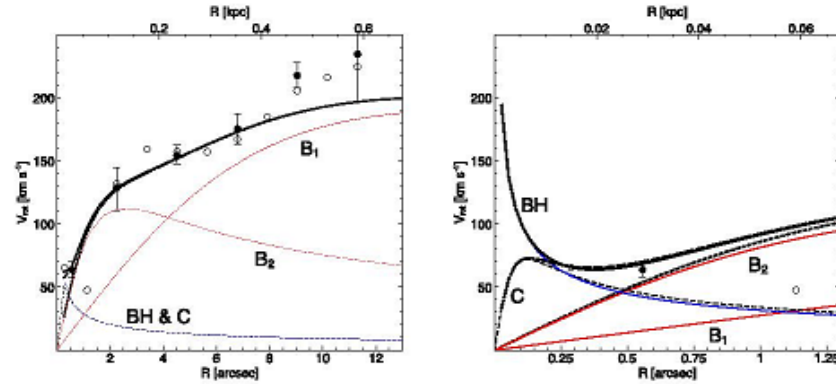
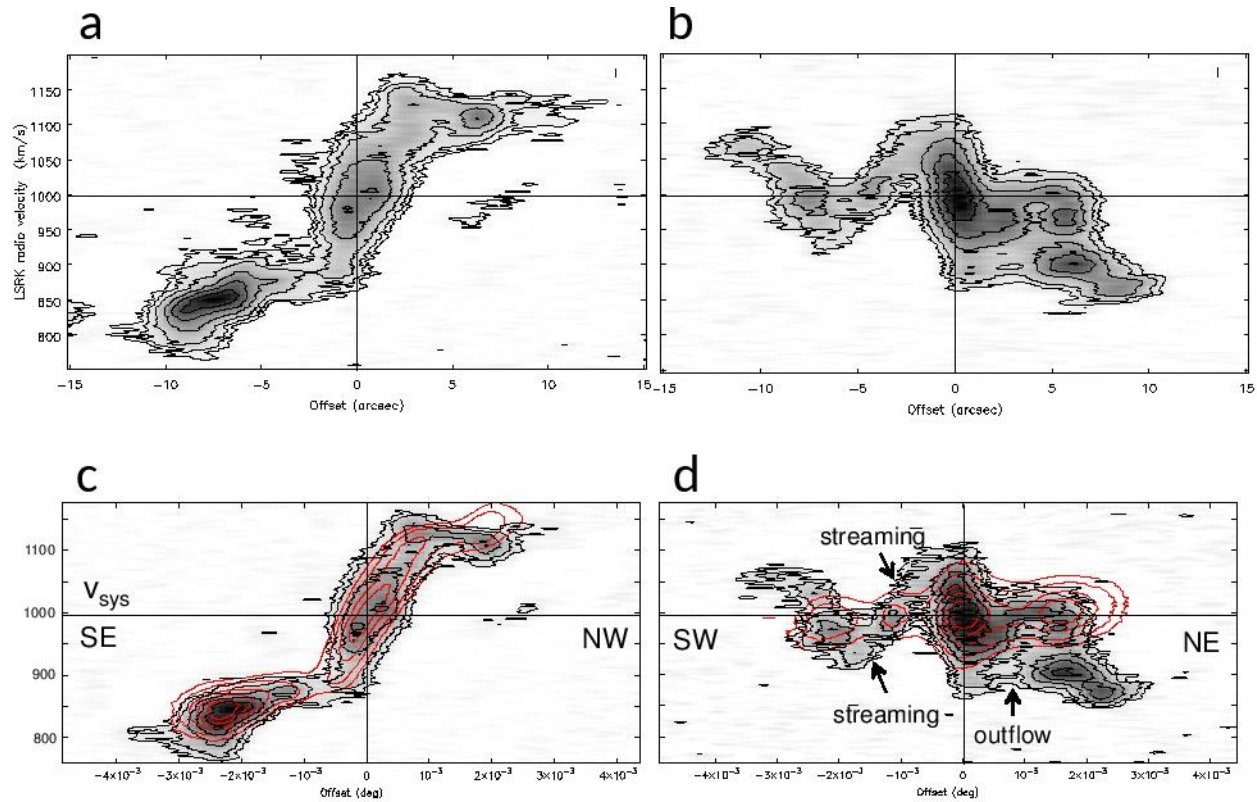


Fig. 20.— *Left.* Rotation curve within $R < 676$ pc fitted with three Plummer spheres and a black hole (Keplerian rotation). The curves represent: bulge (B_1) and major core (B_2) plotted with red dotted lines, nuclear cluster (C, dashed thin line), black hole (BH, blue dotted line), total curve with B_1 and B_2 only (dotted thick line), total curve including C (dashed thick line), and total curve including BH (full thick line). The open circles are the data from figure 19, while the filled circles are the data from the smoothed curve. *Right.* Enlargement of the central 68 pc of the diagram in the left panel.

Table 7: Dynamical parameters of the galactic model in the central 1 kpc.

Component	$\mathcal{M} [M_\odot]$	a [pc]	$\Sigma_s(0) [M_\odot \text{ pc}^{-2}]$
Bulge (B_1)	1.25×10^{10}	575	1.2×10^4
Major core (B_2)	7.2×10^8	95	2.0×10^4
Nuclear bar (NB)	5.8×10^8	95	2.0×10^4
Nuclear cluster (C)	1.4×10^7	4.5	2.20×10^5
Central black hole (BH)	(1.2×10^7)	—	—
Total	1.32×10^{10}		2.52×10^5

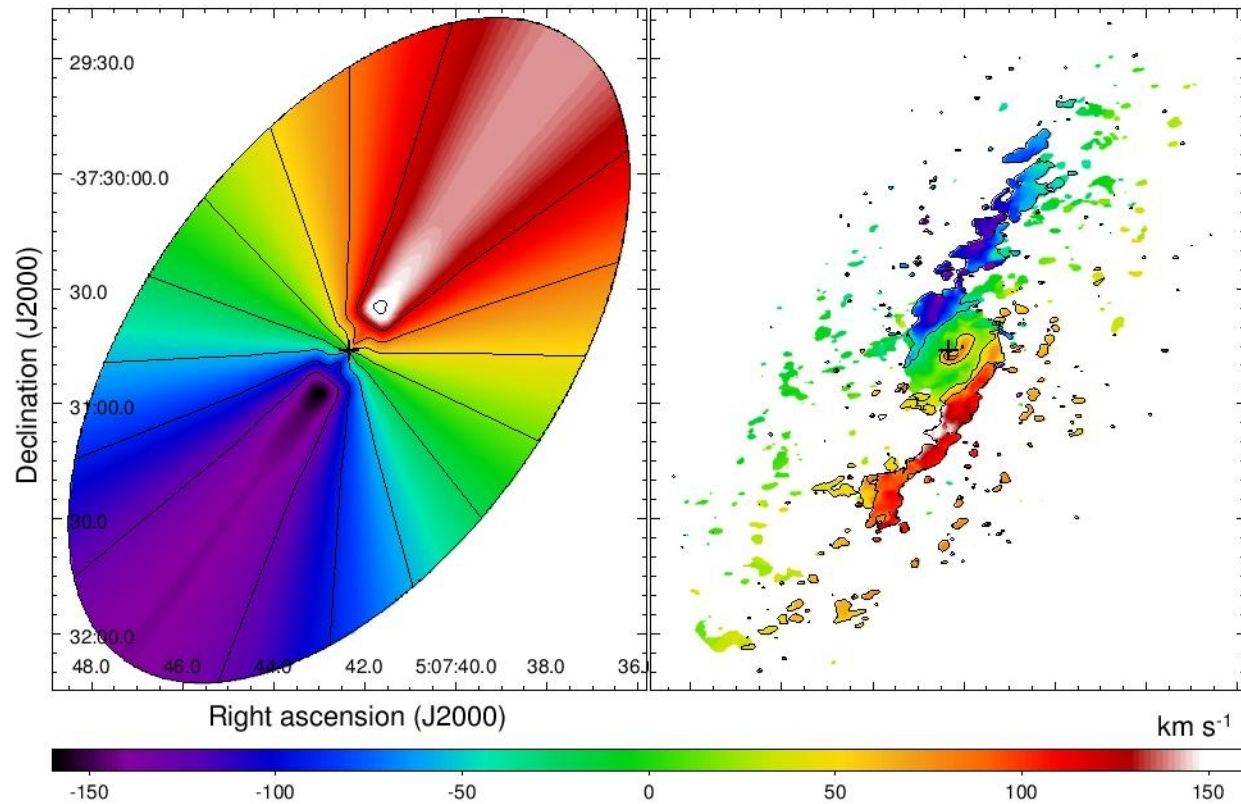
Некруговые движения



Большая ось

Малая ось

Сильные некруговые движения!



Astro-ph: 1603.06295

The Many Assembly Histories of Massive Void Galaxies as Revealed by Integral Field Spectroscopy

Amelia Fraser-McKelvie^{1,2,3*}, Kevin A. Pimbblet^{1,2,3}, Samantha J. Penny⁴ and Michael J. I. Brown^{1,2}.

¹ School of Physics and Astronomy, Monash University, Clayton, Victoria 3800, Australia

² Monash Centre for Astrophysics (MoCA), Monash University, Clayton, Victoria 3800, Australia

³ E. A. Milne Centre for Astrophysics, Department of Physics and Mathematics, University of Hull, Cottingham Road, Kingston-upon-Hull, HU6 7RX, UK

⁴ Institute of Cosmology and Gravitation, University of Portsmouth, Dennis Sciama Building, Burnaby Road, Portsmouth, PO1 3FX, UK

22 March 2016

ABSTRACT

We present the first detailed integral field spectroscopy study of nine central void galaxies with $M_{\star} > 10^{10} M_{\odot}$ using the Wide Field Spectrograph (WiFeS) to determine how a range of assembly histories manifest themselves in the current day Universe. While the majority of these galaxies are evolving secularly, we find a range of morphologies, merger histories and stellar population distributions, though similarly low $H\alpha$ -derived star formation rates ($< 1 M_{\odot} \text{ yr}^{-1}$). Two of our nine galaxies host AGNs, and two have kinematic disruptions to their gas that are not seen in their stellar component.

Массивные галактики, низкие темпы звездообразования

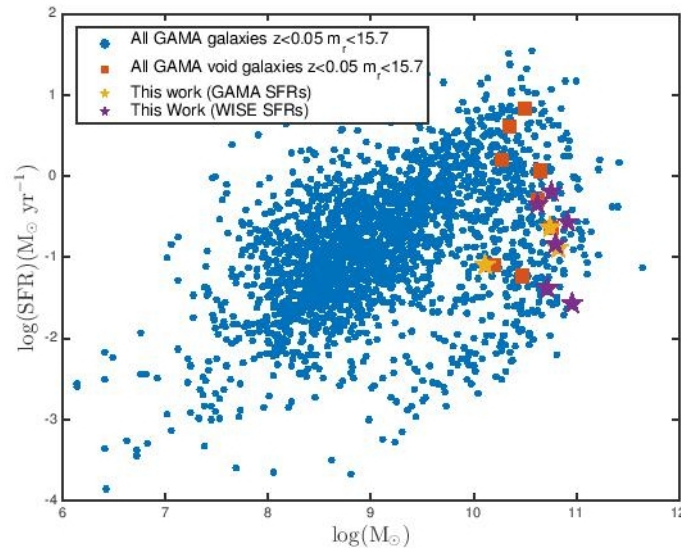


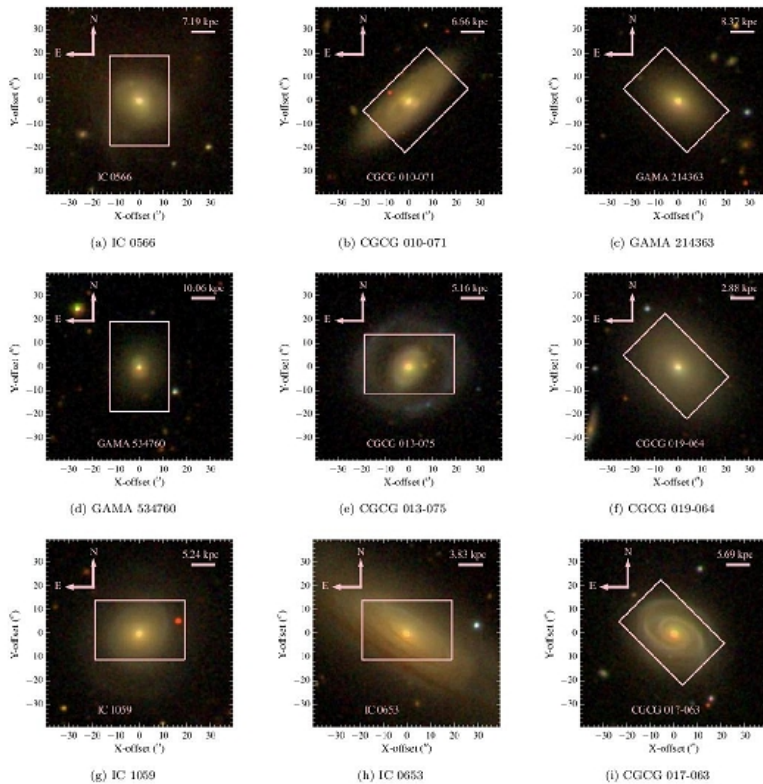
Figure 1. The $H\alpha$ -derived star forming main sequence of all GAMA galaxies with $z < 0.05$. Blue points are all GAMA galaxies, orange are isolated and central void galaxies with $M > 10^{10} M_{\odot}$ from the catalogue of Penny et al. (2015). Yellow points are GAMA galaxies that were observed for this work. Purple points were also observed for this work, but GAMA SFRs were not available, so WISE $W3$ $12\mu\text{m}$ -derived SFRs using the relation of Cluver et al. (2014) were used instead. The isolated and

Спектроскопия интегрального поля в Сайдинг-Спринг

3 OBSERVATIONS & DATA REDUCTION

Observations were taken over two, six night periods from 2014 March 5th–10th and 2015 March 23th–28th using the Wide Field Spectrograph (WiFeS; [Dopita et al. 2007, 2010](#)) on the Australian National University's 2.3m telescope at Siding Spring Observatory. WiFeS is a dual beam, image slicing IFS with a field of view of $25'' \times 38''$, consisting of $25 \times 1''$ slitlets of $38''$ length. If the data are binned 2×1 in the y direction, the resulting spaxel size is $1'' \times 1''$. The B3000 ($\sim 3500\text{--}5800\text{\AA}$) and R3000 ($\sim 5300\text{--}9000\text{\AA}$) gratings were used along with the RT560 dichroic, resulting in a spectral resolution of $\sigma \simeq 100 \text{ km s}^{-1}$ for both the red and blue arms. This wavelength range for our low- z target sample includes the $H\alpha$, $H\beta$, $H\delta$ and $H\gamma$ Balmer lines, along with forbidden lines [NII], [SII], [OIII], the 4000 \AA break and the

Выборка, поле IFU



(a) An SDSS colour image of the galaxy CGCG 013-075 with SDSS fibre diameter and WiFeS rectangular field of view overlaid in green. While the SDSS fibre catches only the red, passive central bulge region of the galaxy, the WiFeS IFS summed spectra catch the blue spiral arm regions and associated $H\alpha$ emission.

Figure 5. SDSS colour images of the nine void galaxies in the sample with the WiFeS field of view of $25'' \times 38''$ overlaid in pink. All galaxies appear optically red, with the exception of CGCG 013-075, which possesses blue spiral arms. IC 0566 contains a total tail in the South-East corner, likely the result of a recent merger.

BPT-диаграммы

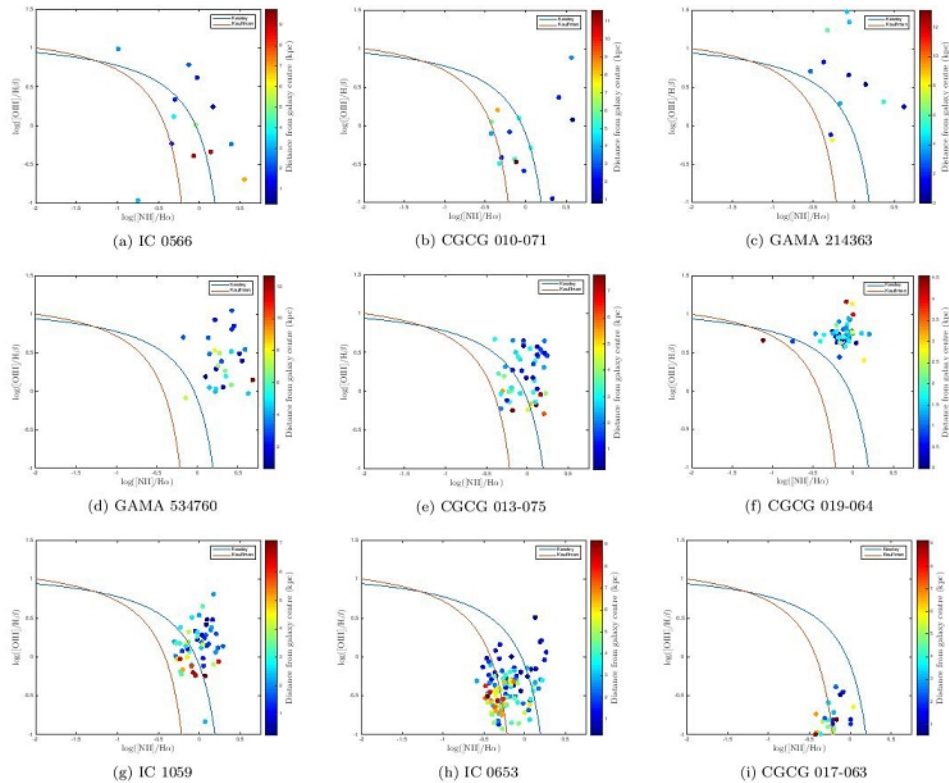


Figure 10. BPT diagrams for sample as a function of distance from galaxy centre for the nine void galaxies studied in this work. The Kauffmann et al. (2003) and Kewley et al. (2006) lines are in orange and blue respectively. We expect CGCG 019-064 to possess an AGN

Профиль темпов звездообразования

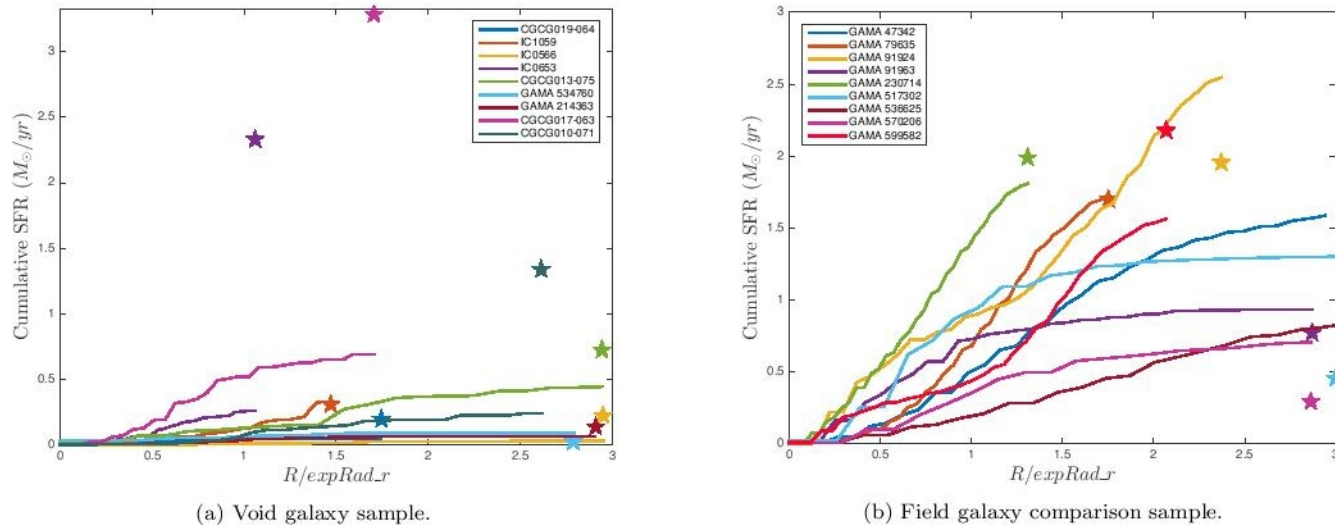


Figure 13. Cumulative $H\alpha$ -derived star formation rates for the nine galaxies in the void galaxy sample and the SAMI comparison sample (coloured lines) and WISE $W3$ total integrated SFRs (stars) where available. All integrated star formation rates are calculated to be $< 1M_{\odot} \text{ yr}^{-1}$ for the void galaxy sample, and $< 3M_{\odot} \text{ yr}^{-1}$ for the SAMI sample, truncated at $3 \times expRad_r$, where required. While on average, the field galaxy integrated SFRs are higher, flux calibration issues and disc regions missed due to low S:N of the void galaxy sample should be taken into account. The two galaxies with the highest discrepancies between $H\alpha$ and WISE $W3$ SFRs were only observed out to 1 and 1.5 $expRad_r$. The superior S:N of the SAMI galaxies means they are often measured out past 2 $expRad_r$. When instead the WISE $12\mu\text{m}$ SFRs are compared, both samples have a very similar spread in SFR, leading us to conclude there is no significant difference between the void and field sample SFRs..